Science Letters Journal

Sci. Lett. J. 2016, 5: 237

ISSN 2454 - 7239

Synthesis, spectroscopic analysis and molecular docking studies of 4-chloro-3-methylphenyl quinoline-2-carboxylate

Fazal Edakot[a], Shana Parveen S[b], Monirah A. Al-Alshaikh[c], C. Yohannan Panicker[b,*], Ali A. El-Emam[d], Subban Nagarajan[e]

[a] *Department of Studies in Chemistry, University of Mysore, Mysore-570 005, India*
[b] *Department of Physics, TKM College of Arts and Science, Kollam, Kerala, India.*
[c] *Department of Chemistry, College of Science, King Saud University, Riyadh 11451, Saudi Arabia*
[d] *Department of Pharmaceutical Chemistry, College of Pharmacy, King Saud University, Riyadh 11451, Saudi Arabia*
[e] *Spice and Flavor Science Department, CSIR-Central Food Technological Research Institute, Mysore, India*

[*] *Author for correspondence: C. Yohannan Panicker, email: cyphyp@rediffmail.com*
Received 05 Mar 2016; Accepted 26 Apr 2016; Available Online 26 Apr 2016

Abstract

The prepared 4-chloro-3-methylphenyl quinoline-2-carboxylate has been investigated by both experimental and theoretical methods, by FT-IR, FT-Raman and NMR techniques. The stability of the strucutre and entire calculations has been performed by DFT method. Potential energy distributions of normal modes of vibrations connected with the vibrations are accomplished applying GAR2PED program. Natural bonding orbital assessment has been completed with a reason to clarify charge transfer or conjugative interaction, the intramolecule rehybridization and delocalization of electron density within the molecule. NMR spectral assessment had been made with choosing structure property relationship by chemical shifts along with magnetic shielding effects regarding the title compound. The hyperpolarizability values, Molecular electrostatic potential, HOMO-LUMO analysis were reported. The docked ligand title compound forms a stable complex with CDK inhibitors and gives a binding affinity value of -7.2 and the results suggest that the title compound might exhibit inhibitory activity against CDK inhibitors.

Keywords: DFT; quinoline; FT-IR; FT-Raman; Molecular docking

1. Introduction

Quinoline compounds are widely used as parental compounds to synthesize molecules with medical benefits, especially with anti-malarial and anti-microbial activities [1-3] and the quinoline ring system containing drugs such as quinine, chloroquine, mefloquine, and amodiaquine are used as efficient drugs for the treatment of malaria [4]. 1,2,3,4-Tetrahydroquinolines are ubiquitous in numerous biologically active natural products and pharmacologically relevant therapeutic agents [5, 6]. Quinoline derivatives in general are known to have a variety of pharmacological and biological activities, such as immunodepresant activity [7] and antitubercular activity [3]. A few reports have been presented in literature on the use of quinoline and some of its derivatives as corrosion inhibitors in different media [8-12]. Optically active substituted tetrahydroquinolines constitute the principal structural unit of many natural alkaloids which display a wide range of physiological activities [13]. In addition, they are very useful synthetic intermediates for the preparation of biologically active compounds for pharmaceutical, agrochemical and fine chemical industries [14]. Some derivatives of 2-oxoquinoline have shown biological activities such as antioxidation, antiproliferation, anti-inflammation and anticancer [15-18]. The vibrational spectroscopic studies of a number of quinoline derivatives are reported in literature [19-27]. To the best of our knowledge, a detailed description of the spectroscopic analysis and theoretical quantum chemical calculations along with nonlinear optical properties has not been given to date for the title compound. Molecular docking studies of the title compound are also reported due to the different potential biological activities of the title compound.

2. Experimental Details

The title compound was synthesized as reported in literature [28]. To a mixture of 1.73g (10 mmol) of quinaldic acid and 10 mmol of 4-Chloro-3-methylphenolin a round-bottomed flask fitted with a reflux condenser with a drying tube is added 0.75g (5 mmol) of phosphorous oxychloride and was subjected to microwave irradiation at 80 °C for 10 minutes using a radiation of 500W (Scheme 1). At the end, the reaction mixture is poured in to a solution of 2g of sodium bicarbonate in 100 mL of water. The precipitated ester is

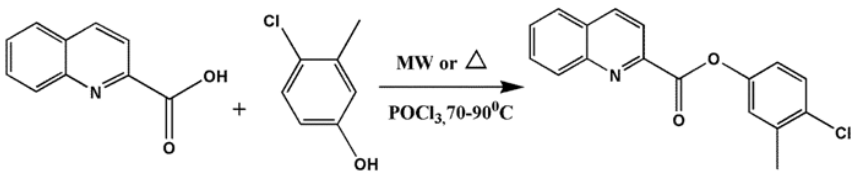

Scheme 1.

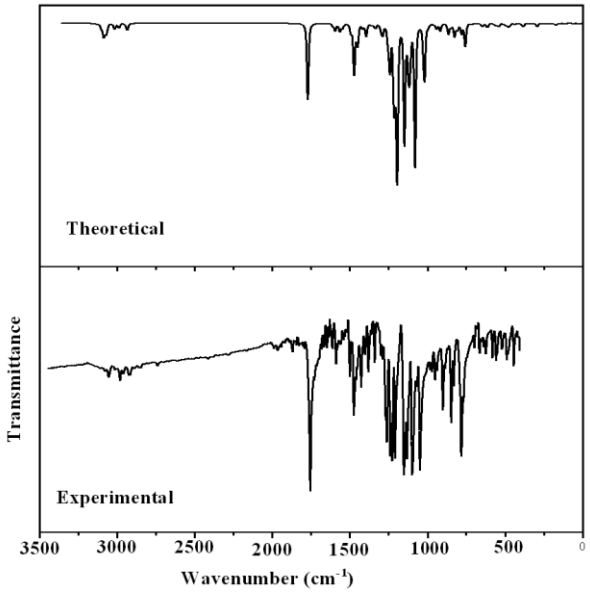

Figure 1. FT-IR spectrum of 4-chloro-3-methylphenyl quinoline-2-carboxylate.

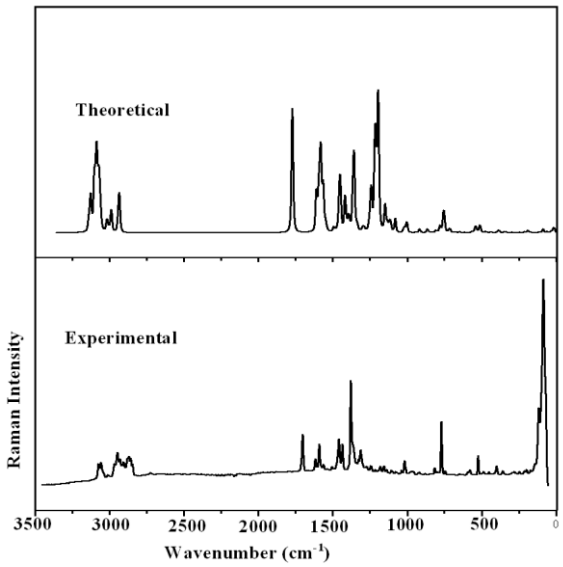

Figure 2. FT-Raman spectrum of 4-chloro-3-methylphenyl quinoline-2-carboxylate.

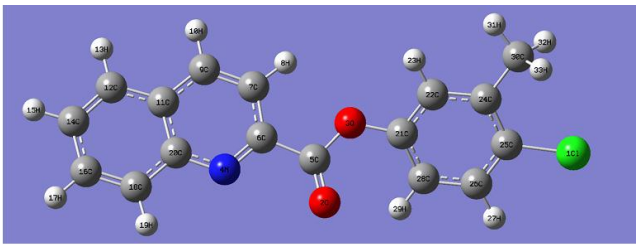

Figure 3. Optimized geometry of 4-chloro-3-methylphenyl quinoline-2-carboxylate.

collected on a filter and washed with water and recrystallized in ethanol. Infrared spectrum (Figure 1) was recorded on a Shimadzu IR prestige-21 FT spectrophotometer with KBr pellets (4000-400 cm^{-1}). The FT-Raman spectrum (Figure 2) was obtained on a Bruker RFS 100/s, Germany. For excitation of the spectrum, the emission of Nd:YAG laser was used with an excitation wavelength of 1064 nm, maximal power 150 mW; measurement on solid sample. One thousand scans were accumulated with a total registration time of about 30 min. The spectral resolution after apodization was 2 cm^{-1}. Elemental analyses were recorded on Varioel elemental analyzer (Elementar Americas, Inc. NJ, USA). NMR spectra (^{1}H and ^{13}C) for the compound were recorded on a 500MHz NMR Spectrometer (Bruker advance, Reinstetten, Germany) using deuteriated DMSO and methanol as the solvent. The chemical shift values (ppm) and coupling constants (J) are given in δ and Hz respectively. Mass spectral analysis were carried out in the ESI positive mode using MS mass spectrometer (Waters Q-TofUtima, Manchester UK). The crystal structure of the title compound is reported by Fazal et al. [29]. In the compound, the dihedral angle between the mean planes of the quinoline ring system and the benzene ring is 68.7(7)°. The mean plane of the carboxylate group is twisted from the latter planes by 14.0(1)° and 80.2(4)°, respectively. In the crystal, weak C-H…O interactions are observed, forming chains along [001]. In addition, π-π stacking interactions [centroid–centroid distances = 3.8343 (13) and 3.7372 (13) Å] occur. MP: 383-385K., Calculated: (C, 68.58; H, 4.06; Cl, 11.91; N, 4.70; O, 10.75) Found: (C, 68.58; H, 4.06; Cl, 11.90; N, 4.71; O, 10.76). MS: Mass (ESI): [M+1] for $C_{17}H_{12}ClNO_2$, Calculated: 297.06; Found: 297.64 and 299.54.

3. Computational Details

In the present work, the density functional theory (B3LYP) at 6-31G(d) (6D, 7F) basis set was adopted to calculated the vibrational wave numbers of the title compound and the theoretical calculations were performed using the Gaussian09 program [30]. Vibrational wavenumbers were computed at DFT level which has reliable one to one correspondence to experimental values and in the present study we have used the scaling factor 0.9613 for the DFT method [31]. At the optimized structure (Figure 3) of the title compound, no imaginary wavenumber modes were obtained. The calculated geometrical parameters are given in Table 1. The vibrational assignments are done with the help of PED analysis and Guassview software [32]. The potential energy distribution is calculated with the help of GAR2PED software package [33].

4. Results and Discussion

In the following discussion, the trisubstituted phenyl ring, quinoline ring and 1,2-disubstituted phenyl ring are designated as PhI, PhII and PhIII, respectively.

4.1. Geometrical parameters

The C-C bond lengths (DFT/XRD) in the phenyl rings, PhI and PhIII lie in the ranges, 1.3930-1.4030/1.3783-1.4013Å and 1.3756-1.4336/1.3624-1.4243Å and for the title compound, the phenyl rings are a regular hexagon with bond lengths somewhere in between the normal values for a single (1.54Å) and a double (1.33Å) bond [23]. The C-O bond lengths (DFT/XRD) of the title compound, 1.2036/1.1903, 1.3935/1.4102, 1.3750/1.3523Å are in agreement with the reported values of a similar derivative (1.2085/1.1930, 1.3961/1.4108, 1.3498/1.3486Å) [23]. For the title compound, the C-N bond lengths (DFT/XRD) are, 1.3587/1.3653, 1.3207/1.3173Å where as the reported values for a similar

Table 1. Optimized geometrical parameters of 4-chloro-3-methylphenyl quinoline-2-carboxylate with XRD data.

Bond lengths (DFT/XRD) (Å)

Cl1-C25	1.7633/1.7452	O2-C5	1.2036/1.1903
O3-C5	1.3750/1.3523	O3-C21	1.3935/1.4102
N4-C6	1.3207/1.3173	N4-C20	1.3587/1.3653
C5-C6	1.5069/1.5093	C6-C7	1.4223/1.4143
C7-H8	1.0825/0.9300	C7-C9	1.3743/1.3663
C9-H10	1.0875/0.9300	C9-C11	1.4167/1.4113
C11-C12	1.4191/1.4223	C11-C20	1.4336/1.4243
C12-H13	1.0874/0.9300	C12-C14	1.3767/1.3624
C14-H15	1.0865/0.9300	C14-C16	1.4188/1.4184
C16-H17	1.0864/0.9300	C16-C18	1.3756/1.3653
C18-H19	1.0852/0.9300	C18-C20	1.4219/1.4203
C21-C22	1.3930/1.3783	C21-C28	1.3936/1.3803
C22-H23	1.0858/0.9300	C22-C24	1.3991/1.4013
C24-C25	1.4030/1.3903	C24-C30	1.5072/1.5013
C25-C26	1.3933/1.3833	C26-H27	1.0846/0.9300
C26-C28	1.3937/1.3913	C28-H29	1.0816/0.9300
C30-H31	1.0937/0.9600	C30-H32	1.0962 /0.9600
C30-H33	1.0960/0.9600		

Bond angles (DFT/XRD) (˚)

C5-O3-C21	121.3/116.3	C6-N4-C20	118.3/117.3
O2-C5-O3	124.4/123.8	O2-C5-C6	125.5/125.7
O3-C5-C6	110.0/110.5	N4-C6-C5	114.7/114.5
N4-C6-C7	123.7/124.7	C5-C6-C7	121.6/120.7
C6-C7-H8	120.0/120.9	C6-C7-C9	118.5/118.1
H8-C7-C9	121.5/120.9	C7-C9-H10	120.7/120.1
C7-C9-C11	119.7/119.8	H10-C9-C11	119.5/120.1
C9-C11-C12	123.6/123.2	C9-C11-C20	117.2/117.5
C12-C11-C20	119.2/119.3	C11-C12-H13	119.0/120.0
C11-C12-C14	120.3/119.9	H13-C12-C14	120.7/120.0
C12-C14-H15	120.0/119.6	C12-C14-C16	120.6/120.9
H15-C14-C16	119.5/119.6	C14-C16-H17	119.4/119.8
C14-C16-C18	120.6/120.5	H17-C16-C18	120.1/119.8
C16-C18-H19	122.1/119.8	C16-C18-C20	120.3/120.3
H19-C18-C20	117.6/119.8	N4-C20-C11	122.5/122.5
N4-C20-C18	118.3/118.5	C11-C20-C18	119.1/119.0
O3-C21-C22	115.5/118.0	O3-C21-C28	120.0/119.6
C22-C21-C28	121.0/122.3	C21-C22-H23	118.7/119.8
C21-C22-C24	121.4/120.4	H23-C22-C24	119.9/119.8
C22-C24-C25	116.9/116.6	C22-C24-C30	120.7/121.1
C25-C24-C30	122.4/122.3	Cl1-C25-C24	119.7/118.7
Cl1-C25-C26	118.3/118.1	C24-C25-C26	122.0/123.2
C25-C26-H27	119.6/120.4	C25-C26-C28	120.3/119.2
H27-C26-C28	120.1/120.4	C21-C28-C26	118.4/118.3
C21-C28-H29	121.0/120.9	C26-C28-H29	120.6/120.9
C24-C30-H31	110.8/109.5	C24-C30-H32	111.3/109.5
C24-C30-H33	111.3 /109.5	H31-C30-H32	108.3/109.5
H31-C30-H33	108.3 /109.5	H32-C30-H33	106.8/109.5

Dihedral angles (DFT/XRD) (˚)

Cl1-C25-C26-C28	-179.9/-179.6	O2-C5-C6-N4	1.8/-13.1
O2-C5-C6-C7	178.1/168.7	O3-C5-C6-N4	178.2/166.5
O3-C5-C6-C7	2.0/11.7	O3-C21-C22-C24	-176.3/-177.1
O3-C21-C28-C26	176.2/176.7	N4-C6-C7-C9	-0.0/-2.7
C5-O3-C21-C22	-139.5/-102.0	C5-O3-C21-C28	44.5/81.7
C5-C6-C7-C9	179.8/175.3	C6-N4-C20-C11	0.2/-0.1
C6-N4-C20-C18	179.9/178.7	C6-C7-C9-C11	0.1/-0.4
C7-C9-C11-C12	-179.9/-176.5	C7-C9-C11-C20	-0.1/2.9
C9-C11-C12-C14	179.9/179.0	C9-C11-C20-N4	-0.1/-2.8
C9-C11-C20-C18	179.9/178.5	C11-C12-C14-C16	-0.0/1.9
C12-C11-C20-N4	179.9/176.7	C12-C11-C20-C18	-0.0/-2.0
C12-C14-C16-C18	-0.0/-0.8	C14-C16-C18-C20	0.0/-1.7
C16-C18-C20-N4	-180.0/175.7	C16-C18-C20-C11	0.0/3.1

Table 1. Optimized geometrical parameters of 4-chloro-3-methylphenyl quinoline-2-carboxylate with XRD data. (Continued)

C20-N4-C6-C5	-180.0/-175.2	C20-N4-C6-C7	-0.1/2.9
C20-C11-C12-C14	0.0/-0.4	C21-O3-C5-O2	-0.3/0.7
C21-O3-C5-C6	179.6/178.9	C21-C22-C24-C25	-0.1/0.3
C21-C22-C24-C30	-180.0/-179.1	C22-C21-C28-C26	0.3/0.6
C22-C24-C25-Cl1	-179.9/-179.2	C22-C24-C25-C26	0.1/0.6
C24-C25-C26-C28	0.0/-0.9	C25-C26-C28-C21	-0.2/0.3
C28-C21-C22-C24	-0.2/-0.9	C30-C24-C25-Cl1	0.0/-1.4
C30-C24-C25-C26	179.9/180.0		

derivative are, 1.3587/1.3626, 1.3156/1.3139Å [23] and these values of C-N bond lengths of the title compound indicate that the bonds show partial double bond character and also the bond distances were found to be much shorter than the average value for a single bond (1.47Å), but significantly longer than a double bond (1.22Å), suggesting some multiple bond character [34]. For the title compound, the C-Cl bond length (DFT/XRD) is 1.7633/1.7452Å where as the reported value for a similar derivative is 1.8304/1.7459Å [24].

At C_{11} position, bond angles (DFT/XRD) are, C_{12}-C_{11}-C_9 = 123.6/123.2, C_9-C_{11}-C_{20} = 117.2/117.5, C_{20}-C_{11}-C_{12} = 119.2/119.3˚ and at C_{20} position, the angles are, C_{11}-C_{20}-C_{18} = 119.1/119.0, C_{18}-C_{20}-N_4 = 118.3/118.5, N_4-C_{20}-C_{11} = 122.5/122.5˚ and this asymmetry gives the interaction between the rings, PhIII and PhII. At the position O_2, the bond angles (DFT/XRD) are, N_4-C_6-C_7 = 123.7/124.7, C_7-C_6-C_5 = 121.6/120.7, C_5-C_6-N_4 = 114.7/114.5˚ and this asymmetry in angles reveals the interaction between O_2 and the ring PhII. Also at the postion C_5, the bond angles are C_6-C_5-O_3 = 110.0/110.5, O_3-C_5-O_2 = 124.4/123.8, O_2-C_5-C_6 = 125.5/125.7˚ which shows the steric repulsion between oxygens atoms O_2 and O_3. The hydrogen bonding between O_3 and H_{23} is revealed by the values of bond angles, C_{22}-C_{21}-C_{28} = 121.0/122.3, C_{28}-C_{21}-O_3 = 120.0/119.6, O_3-C_{21}-C_{22} = 115.8/118.0˚. The rings PhII and PhIII are nearly planar as is evident from the torsion angles, C_{12}-C_{11}-C_9-C_7 = -179.9, C_{12}-C_{11}-C_{20}-N_4 = 179.9, C_{18}-C_{20}-C_{11}-C_9 = 179.9, C_{18}-C_{20}-N_4-C_6 = 179.9˚ whereas the carbonyl group is tilted from the ring PhI as is evident from the torsion angles, C_{22}-C_{21}-O_3-C_5 = -139.5, C_{24}-C_{22}-C_{21}-O_3 = -176.3, C_{26}-C_{28}-C_{21}-O_3 = 176.2, C_{28}-C_{21}-O_3-C_5 = 44.5˚.

4.2. IR and Raman spectra

The observed IR, Raman bands, calculated scaled wave numbers and assignments are given in Table 2. Phenyl ring CH stretching modes are normally expected above 3000 cm^{-1} [35] and in the present case the bands observed at 3105, 3085 cm^{-1} in the IR spectrum and at 3075 cm^{-1} in the Raman spectrum are assigned as these modes. The DFT calculations give these modes in the ranges 3137-3085 and 3126-3073 cm^{-1} for PhI and PhIII rings, respectively. The phenyl ring stretching modes are assigned at, 1595, 1562, 1452, 1401, 1291 (IR), 1594, 1563 (Raman) and 1614, 1546, 1500, 1458, 1364 (IR), 1613, 1501, 1458, 1363 cm^{-1} (Raman) for PhI and PhIII rings, which are expected in the region 1610-1250 cm^{-1} [35].

In ortho disubstitution, the ring breathing mode has three wavenumber intervals depending on whether both substituents are heavy; or one of them is heavy, while the other is light; or both of them are light [36]. In the first case, the interval is 1100-1130 cm^{-1}; in the second case 1020-1070 cm^{-1}; while in the third case it is between 630 and 780 cm^{-1} [36]. For the title compound, ring breathing mode of PhIII is observed at 1075 in the IR spectrum, 1079 in the Raman spectrum and at 1081 cm^{-1} theoretically. The ring breathing mode of ortho substituted benzene ring is reported at 1091 cm^{-1} [37].

In asymmetric trisubstituted benzene, when all the three substituents are light, the ring breathing mode falls in the range 500-600 cm^{-1}, when all the three substituents are heavy it appears above 1100 cm^{-1} and in the case of mixed substituents, it falls in the range 600-750 cm^{-1} [36]. For the title compound, PED analysis gives the ring breathing mode of the tri-substituted benzene at 1122 cm^{-1}. According to literature, the ring breathing mode of tri substituted benzenes are reported at 1110, 1083 cm^{-1} [38] and 1063 cm^{-1} [39].

The in-plane CH deformation modes of the phenyl rings are observed at 1260, 1242, 1152 in the IR spectrum and at 1244, 1152, 1112 cm^{-1} in the Raman spectrum as expected [35] and the DFT calculations give these modes in the ranges 1255-1122 for PhI and 1244-1004 cm^{-1} for PhIII rings. The out-of-plane bending modes of the phenyl rings are assigned at 866, 784, (IR), 804 (Raman) for PhI and 970, 760 cm^{-1} (IR) for PhIII rings, where as the corresponding theoretical values are in the ranges 912-782 for PhI and 966-758 cm^{-1} for PhIII, which are expected below 1000 cm^{-1} according to literature [35].

The CH modes associated with the quinoline ring are assinged at: 3058 (IR), 3058 (Raman), 3067, 3060 (DFT) (stretching), 1132 (IR), 1135 (Raman), 1417, 1134 (DFT) (in-plane bending) and 958, 830 (IR), 958, 822 (Raman), 960, 828 cm^{-1} (DFT) (out-of-plane bending). The methyl stretching modes are expected in the range 2900-3000 cm^{-1} [35] and the bands at 3013, 2988, 2940 (IR), 3013, 2980, 2942 (Raman) and 3016, 2990, 2936 cm^{-1} (DFT) are assigned as methyl stretching modes. The deformation modes of the methyl group are assinged at 1475, 1388, 1037 in the IR spectrum, 1034, 1020 in the Raman spectrum and in the range 1474-1022 cm^{-1} theoretically.

For the title compound, the carbonyl stretching mode is observed at 1760 cm^{-1} in the IR spectrum with a theoretical value 1772 cm^{-1}. The quinoline ring C=C and C=N stretching modes are observed at 1580 and 1546 cm^{-1} in the IR spectrum with computed values 1583 and 1548 cm^{-1} as expected [35, 40, 41]. Inorder to investigate the performance of vibrational wavenumbers of the title compound, the root mean square value between the calculated and observed wavenumbers were calculated and the RMS errors are 3.56 for IR and 3.79 for Raman modes.

4.3. NMR spectra

The chemical informationof the molecular components of the compound can be extracted from the experimental chemical shift and it can be found that whether the results are true or not from the calculated data. In this case the experimental data was collected by recording the spectra and the ^1H and ^{13}C NMR spectral data was calculated at B3LYP method with 6-31G(d) (6D, 7F) level on the basis of GIAO method and the chemical shifts were reported in ppm

Table 2. Calculated (scaled) wavenumbers, observed IR, Raman bands and assignments of 4-chloro-3-methylphenyl quinoline-2-carboxylate.

B3LYP/6-31G(d) (6D, 7F)			IR $\upsilon(cm^{-1})$	Raman $\upsilon(cm^{-1})$	Assignments[a]
$\upsilon(cm^{-1})$	IR_I	R_A			
3137	0.58	72.32			υCHI(97)
3126	1.88	111.77			υCHIII(98)
3101	10.08	168.66			υCHIII(97)
3099	2.57	98.19	3105		υCHI(96)
3086	26.58	266.47	3085		υCHIII(99)
3085	5.70	56.41	3085		υCHI(99)
3073	15.23	132.42		3075	υCHIII(93)
3067	9.71	98.74			υCHII(92)
3060	1.26	30.53	3058	3058	υCHII(91)
3016	14.99	56.96	3013	3013	υCH_3(99)
2990	11.08	91.15	2988	1980	υCH_3(99)
2936	18.63	181.11	2940	2942	υCH_3(100)
1772	166.83	332.74	1760		υC=O(80)
1611	4.73	93.30	1614	1613	υPhIII(59), δCHIII(19)
1596	14.16	67.55	1595	1594	υPhI(65), δCHI(15)
1583	3.10	285.31	1580		υC=C(45), υC=N(19), υPhIII(12)
1565	16.75	105.99	1562	1563	υPhI(63), δCHI(15)
1548	11.78	24.63	1546		υC=N(38), υPhIII(40)
1494	19.52	11.76	1500	1501	υPhIII(56), υCCII(17), δCHIII(13)
1474	113.17	3.24	1475		δCH_3(51), δCHI(24)
1454	3.12	105.55	1458	1458	δCH_3(11), δCHIII(10), υPhIII(54)
1452	49.51	73.13	1452		δCH_3(21), δCHI(17), υPhI(57)
1452	8.16	19.62	1452		δCH_3(97)
1417	10.82	102.65			δCHIII(44), δCHII(40)
1396	24.47	24.30	1401		υPhI(57), δCHI(18), δCH_3(14)
1390	2.94	18.47	1388		δCH_3(89)
1361	4.61	274.64	1364	1363	υPhIII(71)
1338	12.98	18.20	1340	1335	υC=N(25), δCHIII(13), υPhIII(16)
1299	18.41	13.89	1302		υCN(37), δCHII(10), δCHIII(21)
1290	20.17	7.19	1291		υPhI(90)
1255	28.17	10.82	1260		δCHI(61)
1244	113.23	116.48	1242	1244	δCHIII(50), υCC(11), υPhIII(10)
1218	26.77	33.22	1222		υPhIII(24), υCC(22), υCCII(25)
1215	229.73	297.47	1212	1214	υCO(18), υPhI(12), υCC(10), δCHI(15)
1196	320.46	297.49		1190	υCC(15), υPhIII(11), δCHII(18), υCCII(10)
1149	245.17	56.69	1152	1152	υCO(42), δCHI(40)
1140	12.81	5.70			δCHIII(65)
1134	3.50	11.56	1132	1135	δCHII(48), δCHII(14), υPhIII(21)
1122	96.59	11.39			δCHI(45), υPhI(41)
1115	105.30	30.48		1112	δCHIII(43), υPhIII(14)
1081	299.13	29.70	1075	1079	υCO(40), υPhIII(44)
1032	3.30	0.72	1037	1034	δCH_3(72)
1022	163.24	14.59		1020	δPhI(40), δCH_3(32)
1004	0.39	22.61			υPhIII(11), δCHIII(69)
996	4.55	1.45			δCH_3(52), υPhI(12), δPhI(11)
966	0.03	0.07	970		γCHIII(87), τPhIII(11)
960	0.92	0.24	958	958	γCHII(85)
944	11.95	1.33	942		δPhII(46), υPhI(16), υCC(14)
933	1.36	0.04			γCHIII(83)
918	16.01	7.61		918	δPhII(30), δPhIII(26)

Table 2. Calculated (scaled) wavenumbers, observed IR, Raman bands and assignments of 4-chloro-3-methylphenyl quinoline-2-carboxylate. (Continued)

912	0.31	1.13			γCHI(84)
866	21.88	5.76	866		γCHI(49), τPhI(21)
862	1.79	3.82			γCHIII(59), τPhIII(12), γCHII(19)
848	7.97	1.12	849		γCHI(31), δPhIII(21)
828	27.59	0.17	830	822	γCHII(56), γCC(10), γCHIII(15)
808	20.23	6.00		804	γCHI(50), δCO(11)
782	21.15	12.87	784		γCHI(61)
776	0.52	2.38		774	τPhII(44), τPhIII(25), γCC(10)
758	44.85	5.43	760		γCHIII(61), γC=O(21)
754	4.43	58.40		752	δPhIII(49), δCC(11), δPhII(13)
717	2.06	5.99			δPhI(34), γC=O(28), τPhIII(22)
714	0.18	5.83			γC=O(18), τPhIII(13), γCHIII(22), γCHII(21)
677	0.60	1.89	672		τPhI(63), γCCl(11), γCO(19)
647	7.79	2.67	642		δPhI(26). υCCl(38), τPhI(10)
618	5.26	0.32	620		τPhII(23), τPhIII(32), γC=O(16)
614	5.98	0.47			δPhII(39), δPhIII(31)
568	3.05	2.12		572	δPhIII(24), τPhI(10), γCO(10)
554	5.25	2.25	556		τPhI(25), γCO(24), γCC(12), γCCl(11)
539	7.54	17.06		530	δPhI(40), δCCl(17)
513	1.12	15.46	510		δPhII(37), δPhIII(44)
496	3.43	0.30			τPhII(27), τPhIII(46)
482	6.54	1.19	480	484	δCC(22), δPhIII(19), δC=O(22)
473	2.06	1.40			τPhII(45), τPhIII(28)
467	2.09	1.13		460	δCC(26), δCO(15), τPhIII(20)
438	2.72	1.96	440		τPhI(65), γCC(14)
392	2.06	3.56			τPhII(38), τPhIII(39)
383	7.68	5.15			δPhI(18), δCO(10), γCCl(22)
348	0.47	1.86		350	δPhII(36), δC=O(32)
335	0.69	1.90			γCCl(35), τPhI(21)
294	8.07	1.21			δCC(27), δCO(37)
248	0.54	0.51		248	τPhIII(36), γCC(18)
239	0.65	0.66			δCCl(56), δCC(20)
212	0.89	1.81			τPhI(16), γCC(15), γCCl(17)
190	1.28	5.75		192	δCC(24), δCO(22)
173	3.20	0.21		171	τPhII(50), τPhIII(36)
163	0.58	0.59			δCO(13), δC=O(22), δPh(17), δPhII(12)
145	0.39	0.32		146	τCH_3(86)
115	0.78	1.13		116	τPhI(37), δCC(12), τCO(17)
88	0.07	6.57		87	τPhII(42), τPhIII(10), τPhI(21)
60	0.53	2.71			τCO(56), τCC(12)
34	0.20	2.94			τCO(36), δCO(29), τCC(16)
20	0.54	3.28			τCO(47), δCO(30)
14	0.24	9.08			τCO(54), δCO(41)

[a]υ-stretching; δ-in-plane bending; γ-out-of-plane bending; τ-torsion; trisubstituted phenyl ring-PhI; Quinoline ring-PhII; 1,2-disubstituted phenyl ring-PhIII; potential energy distribution (%) is given in brackets in the assignment column.

relative to TMS. The NMR spectral data were presented in Table 4 and the corresponding spectra were shown Figures 4 and 5.

The experimental NMR data are: ^{1}HNMR (500MHz, DMSO, δ): 8.66 (1H, d, J= 8.51Hz), 8.27(1H, d, J= 8.5Hz), 8.24(1H, d, J= 8.43 Hz), 8.15(1H, d, J= 8.2 Hz), 7.93(1H, dt, J_1= 8.07Hz, J_2=6.73, J_3=1.06Hz), 7.8(1H, t, J= 7.55Hz), 7.54(1H, d, J= 8.6Hz), 7.41(1H, d, J= 2.4Hz), 7.26(1H, dd, J_1= 8.6Hz, J_2=2.57 Hz), 3.3-3.4(1H, m), 2.38(3H, s).

^{13}CNMR (125 MHz, DMSO, δ): 19.787, 121.328, 121.446, 124.668, 128.272, 129.962, 130.051, 130.733, 131.080, 137.273, 138.128, 146.956, 147.100, 149.499 and 163.636.

In the ^{1}H NMR spectrum of the title compound, the signals due to six aromatic protons of quinoline moiety were appeared in the region 8.66 to 7.8. Three protons on benzene ring appeared as two doublets at 7.54 and 7.41 and a doublet of doublet at 7.26 and the pattern indicate para and meta substitution. Three protons of methyl group are indicated by a singlet at 2.38. The presence of carbonyl carbon assured by the

Table 3. The predicted ^{1}H and ^{13}C NMR isotropic chemical shifts (with respect to TMS, all values in ppm).

Atom	σ_{TMS}	B3LYP/6-31G(d) (6D, 7F) σ_{calc}	δ_{calc} (σ_{TMS} - σ_{calc})
H8	32.7711	24.0150	8.7561
H10		24.2483	8.5228
H13		24.5098	8.2613
H15		24.5752	8.1959
H17		24.4152	8.3559
H19		23.9427	8.8284
H23		25.4181	7.353
H27		25.0333	7.7378
H29		24.6956	8.0755
H31		30.3699	2.4012
H32		29.7745	2.9966
H33		29.7582	3.0129
C5	189.6900	38.2716	151.4184
C6		48.0232	141.6668
C7		73.2972	116.3928
C9		60.1783	129.5117
C11		67.6718	122.0182
C12		68.4548	121.2352
C14		67.1682	122.5218
C16		66.6146	123.0754
C18		62.9196	126.7704
C20		47.6646	142.0254
C21		46.8757	142.8143
C22		73.3838	116.3062
C24		58.4822	131.2078
C25		56.7224	132.9676
C26		66.2074	123.4826
C28		74.4950	115.195
C30		167.9308	21.1752

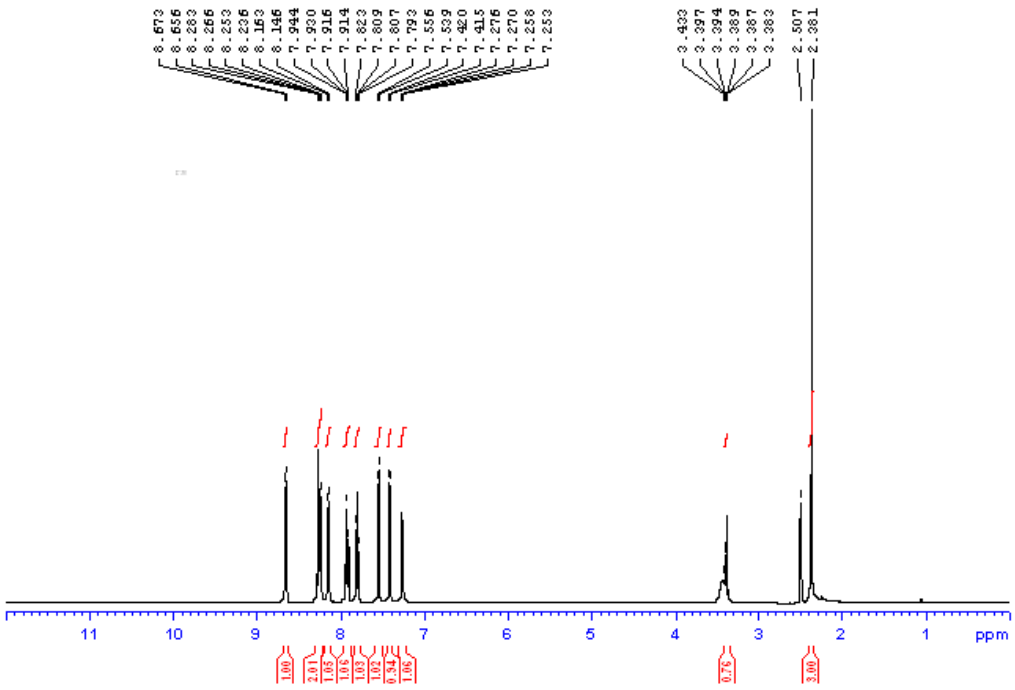

Figure 4. ^{1}H NMR spectrum of 4-chloro-3-methylphenyl quinoline-2-carboxylate.

presence of a signal at 163.636 in ^{13}C NMR spectrum and a signal at 19.787 confirms the presence of meta methyl group on benzene ring. The molecular ion peak at m/z 298 present in the electrospray ionization mass spectrum of the title compound in positive mode along with isotopic peak (M+2) due to chlorine is consistent with the molecular formula $C_{17}H_{12}ClNO_2$.

4.4. Nonlinear optical properties

Polarizability and hyperpolarizability characterize the response of a system to an applied electric field [42-44] and

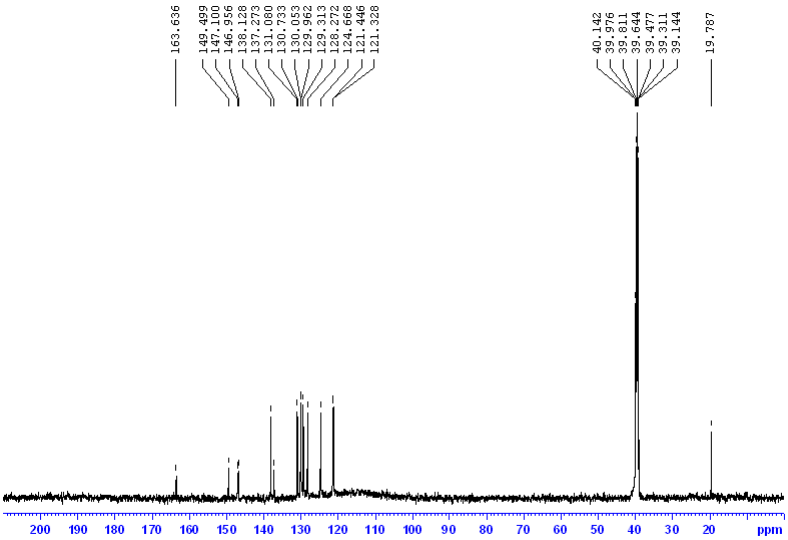

Figure 5. ^{13}C NMR spectrum of 4-chloro-3-methylphenyl quinoline-2-carboxylate.

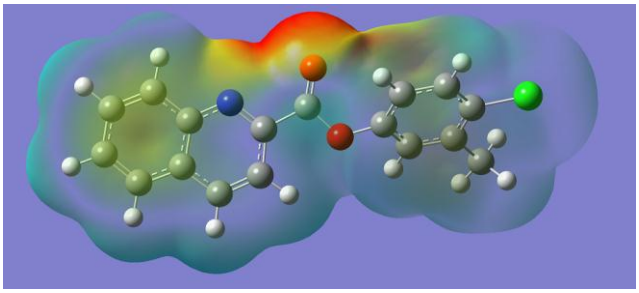

Figure 6. MEP plot of 4-chloro-3-methylphenyl quinoline-2-carboxylate.

these terms are essential to analyze the nonlinear optical properties of materials. For the title compound the theoretically calculated values of dipole moment and polarizability are 1.958 Debye and 3.131×10^{-23} esu, respectively. The calculated first hyperpolarizability of the title compound is 3.254×10^{-30} e.s.u which is 25.03 times that of the standard NLO material urea (0.13×10^{-30} e.s.u) [45]. The average second hyperpolarizability has been calculated by using the following expression.

$$\gamma_{av} = 1/5[\gamma_{xxxx} + \gamma_{yyyy} + \gamma_{zzzz} + 2\gamma_{xxyy} + 2\gamma_{xxzz} + 2\gamma_{yyzz}]$$

The amount of charge transfer for the molecule depends on the nature of the end group of the molecule and the increase of π-conjugated chain length in organic molecules, in general, enhances the magnitude of hyperpolarizability. The calculated value of γ_{av} for the title compound is -24.131×10^{-37} esu. The larger component of second hyperpolarizability is associated with the larger ground state polarization which leads to strong electronic coupling between the ground and the low lying excited state and this can be attributed to the enhanced charge transfer interaction taking place. Thus, the present investigation provides a new route to design high performance NLO materials.

4.5. Molecular Electrostatic Potenital

Molecular electrostatic potential is related to the electron density and is very useful in predicting the sites for electrophilic attack, nucleophilic reactions and hydrogen bonding interactions [46, 47]. The different values of the electrostatic potential at the surface are represented by different colours. Red region indicates the most electronegative electrostatic potential (electrophilic), blue region indicates the most positive electrostatic potential (nucleophilic) and green region represents the zero potential. The electrostatic potential increases in the order red < orange < yellow < green < blue [48]. The mapped electrosatic potential surface has been plotted for the titlecompound and shown in Figure 6. The negative regions are over the carbonyl group oxygen atom and hene electrophilic attack can take place in these sites. The positive regions are over the hydrogen atoms hence nucleophilic attack can take place in these regions.

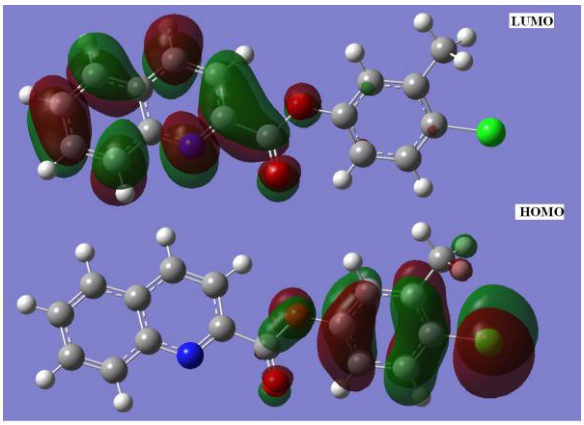

Figure 7. HOMO, LUMO plots of 4-chloro-3-methylphenyl quinoline-2-carboxylate.

4.6. Frontier Molecular Orbitals

The highest occupied molecular orbital (HOMO) and the lowest unoccupied molecular orbital (LUMO) are the main orbitals taking part in the chemical stability. The HOMO and LUMO represents the ability of donating and accepting an electron respetively. The frontier molecular orbtials and the energy gap are very useful in studying the reactivity and kinetic stability, which are important parameters in analyzing its electronic properties [49-51]. The energy needed to remove an electron from the filled orbital is known as ionization energy, which is obtained as $I = -E_{HOMO}$, the energy released when an electron is added to an unfilled orbital is termed as electron affinity, which is calculated as $A = -E_{LUMO}$. Figure 7 shows the frontier molecular orbitals. Using the HOMO and LUMO orbital energies, the ionization energy and electron

Table 4. Second-order perturbation theory analysis of Fock matrix in NBO basis corresponding to the intramolecular bonds of the title compound.

Donor(i)	Type	ED/e	Acceptor(j)	Type	ED/e	E(2)[a]	E(j)-E(i)[b]	F(i,j)[c]
O2-C5	σ	1.99675	C5-C6	σ*	0.08031	1.43	1.50	0.042
	π	1.98211	N4-C6	π*	0.34393	4.17	0.39	0.039
O3-C5	σ	1.98862	N4-C6	σ*	0.01635	1.48	1.46	0.042
			C21-C22	σ*	0.02138	1.46	1.47	0.041
C5-C6	σ	1.97361	O3-C21	σ*	0.03678	3.49	0.99	0.053
			N4-C20	σ*	0.01972	4.01	1.18	0.061
			C6-C7	σ*	0.03473	1.19	1.19	0.034
			C7-C9	σ*	0.01324	1.77	1.27	0.042
C6-C7	σ	1.98101	O2-C5	σ*	0.01648	1.84	1.32	0.044
			N4-C6	σ*	0.01635	2.19	1.27	0.047
			C5-C6	σ*	0.08031	1.11	1.10	0.032
			C7-C9	σ*	0.01324	2.30	1.30	0.049
C11-C20	σ	1.97219	N4-C20	σ*	0.01972	1.25	1.19	0.035
			C9-C11	σ*	0.02188	2.57	1.22	0.050
			C11-C12	σ*	0.02211	2.92	1.23	0.053
			C18-C20	σ*	0.02504	2.69	1.22	0.051
C18-C20	σ	1.97643	N4-C6	σ*	0.01635	2.74	1.25	0.052
			N4-C20	σ*	0.01972	1.70	1.19	0.040
			C9-C11	σ*	0.02188	2.40	1.22	0.048
			C11-C20	σ*	0.04342	2.65	1.21	0.051
			C16-C18	σ*	0.01322	2.27	1.29	0.048
C21-C22	σ	1.97659	O3-C5	σ*	0.12029	1.99	1.05	0.042
			C21-C28	σ*	0.02682	3.76	1.28	0.062
			C22-C24	σ*	0.02039	2.80	1.29	0.054
			C24-C30	σ*	0.01487	1.02	0.60	0.023
			C24-C25	π*	0.40990	21.65	0.28	0.071
			C26-C28	π*	0.33272	19.09	0.29	0.067
C21-C28	σ	1.97932	C21-C22	σ*	0.02138	3.93	1.28	0.063
			C26-C28	σ*	0.01571	2.34	1.29	0.049
C24-C25	σ	1.97706	C22-C24	σ*	0.02039	2.99	1.29	0.056
			C24-C30	σ*	0.01487	2.19	1.13	0.045
			C25-C26	σ*	0.02444	3.90	1.28	0.063
	π	1.66320	C21-C22	π*	0.38003	17.89	0.29	0.065
			C26-C28	π*	0.33272	21.44	0.29	0.071
C25-C26	σ	1.98087	C24-C25	σ*	0.03518	4.38	1.28	0.067
			C24-C30	σ*	0.01487	3.13	1.14	0.053
			C26-C28	σ*	0.01571	2.48	1.30	0.051
LPCl1	σ	1.99367	C24-C25	σ*	0.03518	1.20	1.47	0.038
			C25-C26	σ*	0.02444	1.14	1.48	0.037
	π	1.97151	C24-C25	σ*	0.03518	4.20	0.87	0.054
			C25-C26	σ*	0.02444	3.47	0.88	0.049
	n	1.93332	C24-C25	π*	0.40990	11.31	0.33	0.060
LPO2	σ	1.97728	O3-C5	σ*	0.12029	1.46	1.02	0.035
			C5-C6	σ*	0.08031	2.82	1.08	0.050
	π	1.82886	O3-C5	σ*	0.12029	38.06	0.60	0.136
			C5-C6	σ*	0.08031	20.16	0.66	0.105
LPO3	σ	1.95025	O2-C5	σ*	0.01648	2.19	0.57	0.035
			C21-C28	σ*	0.02682	4.97	1.11	0.067
	π	1.78653	O2-C5	π*	0.22595	41.37	0.35	0.107
			C21-C22	σ*	0.02138	2.04	0.91	0.040
			C21-C22	π*	0.38003	13.82	0.36	0.066
			C21-C28	σ*	0.02682	2.14	0.90	0.041
LPN4	σ	1.91786	C5-C6	σ*	0.08031	3.42	0.74	0.045
			C6-C7	σ*	0.03473	10.97	0.86	0.088
			C11-C20	σ*	0.04342	10.80	0.86	0.087
			C18-C20	σ*	0.02504	1.87	0.88	0.037

[a]E(2) means energy of hyper-conjugative interactions (stabilization energy in kJ/mol)
[b]Energy difference (a.u) between donor and acceptor i and j NBO orbitals
[c]F(i,j) is the Fock matrix elements (a.u) between i and j NBO orbitals

Table 5. NBO results showing the formation of Lewis and non-Lewis orbitals.

Bond(A-B)	ED/e[a]	EDA%	EDB%	NBO	s%	p%
σO2-C5	1.99675 -1.10014	65.73	34.27	0.8107($sp^{1.36}$)O+ 0.5854($sp^{1.89}$)C	42.35 34.55	57.65 65.45
σO3-C5	1.98862 -0.90183	69.99	30.01	0.8366($sp^{2.16}$)O+ 0.5478($sp^{2.70}$)C	31.63 26.98	68.37 73.02
σC5-C6	1.97361 -0.66963	48.37	51.63	0.6955($sp^{1.60}$)C+ 0.7186($sp^{2.32}$)C	38.47 30.12	61.53 69.88
σC6-C7	1.98101 -0.70452	50.29	49.71	0.7091($sp^{1.63}$)C+ 0.7051($sp^{2.03}$)C	38.05 32.99	61.95 67.01
σC11-C20	1.97528 -0.69255	50.92	49.08	0.7136($sp^{2.14}$)C+ 0.7006($sp^{1.85}$)C	31.85 35.04	68.15 64.96
σC18-C20	1.97643 -0.68407	48.94	51.06	0.6996($sp^{1.98}$)C+ 0.7146($sp^{1.88}$)C	33.56 34.76	66.44 65.24
σC21-C22	1.97659 -0.71214	50.19	49.81	0.7084($sp^{1.66}$)C+ 0.7058($sp^{1.88}$)C	37.52 34.72	62.48 65.28
σC21-C28	1.97932 -0.71358	50.42	49.58	0.7101($sp^{1.58}$)C+ 0.7041($sp^{1.95}$)C	38.74 33.88	61.26 66.12
σC24-C25	1.97706 -0.71859	50.01	49.99	0.7071($sp^{1.97}$)C+ 0.7071($sp^{1.56}$)C	33.61 39.00	66.39 61.00
πC24-C25	1.66320 -0.26444	45.83	54.17	0.6770($sp^{1.00}$)C+ 0.7360($sp^{1.00}$)C	0.00 0.00	100.0 100.0
σC25-C26	1.98087 -0.72213	50.90	49.10	0.7134($sp^{1.56}$)C+ 0.7007($sp^{1.88}$)C	39.02 34.68	60.98 65.32
n1Cl1	1.99367 -0.91366			$sp^{0.22}$	82.24	17.76
n2Cl1	1.97151 -0.31594			$sp^{1.00}$	0.00	100.00
n3Cl1	1.93332 -0.31530			$sp^{1.00}$	0.00	100.00
n1O2	1.97728 -0.68539			$sp^{0.73}$	57.69	42.31
n2O2	1.82886 -0.25769			$sp^{99.99}$	0.02	99.98
n1O3	1.95025 -0.54928			$sp^{1.90}$	34.44	65.56
n2O3	1.78653 -0.33853			$sp^{99.99}$	0.51	99.49
n1N4	1.91786 -0.34039			$sp^{2.53}$	28.28	71.72

[a] ED/e is expressed in a.u.

affinity can be expressed as: $I= -E_{HOMO}$, $A = -E_{LUMO}$. The hardness η and chemical potential μ are given the following relations η = (I-A)/2 and μ = - (I+A)/2, where I and A are the first ionization potential and electron affinity of the chemical species [52]. For the title compound, the E_{HOMO} = -7.901 eV, E_{LUMO} = -5.671 eV, Energy gap = HOMO-LUMO = 2.23 eV, Ionization potential I= 7.901 eV, Electron affinity A = 5.671 eV, global hardness η = 1.115 eV, chemical potential μ = -6.786 eV, global electrophiliciy = $\mu^2/2\eta$ = 20.75 eV. It is seen that the chemical potential of the title compound is negative and it means that the compound is stable.

4.7. Natural Bond Orbital Analysis

The natural bond orbitals (NBO) calculations were performed using NBO 3.1 program [53] the DFT/B3LYP level in order to understand various second-order interactions between the filled orbitals of one subsystem and vacant orbitals of another subsystem and the important results are given in Tables 4 and 5.

The important intra-molecular hyper conjugative interactions are: C_{24}-C_{25} from Cl_1 of $n_1(Cl_1)\rightarrow\sigma^*(C_{24}$-$C_{25})$, C_{24}-C_{25} from Cl_2 of $n_2(Cl_2)\rightarrow\sigma^*(C_{24}$-$C_{25})$, C_{24}-C_{25} from Cl_3 of $n_3(Cl_3)\rightarrow\pi^*(C_{24}$-$C_{25})$, C_5-C_6 from O_2 of $n_1(O_2)\rightarrow\sigma^*(C_5$-$C_6)$, O_3-C_5 from Cl_2 of $n_2(O_2)\rightarrow\sigma^*(O_3$-$C_5)$, C_{21}-C_{28} from O_3 of $n_1(O_3)\rightarrow\sigma^*(C_{21}$-$C_{28})$, O_2-C_5 from O_3 of $n_2(O_3)\rightarrow\pi^*(O_2$-$C_5)$, C_6-C_7 from N_4 of $n_1(N_4)\rightarrow\sigma^*(C_6$-$C_7)$ with electron densities, 0.03518, 0.03518, 0.40990, 0.08031, 0.12029, 0.02682, 0.22595, 0.03473e and stabilization energies, 1.20, 4.20, 11.31, 2.82, 38.06, 4.97, 41.37, 10.97 KJ/mol.

The natural hybrid orbitals with higher energies are: $n_3(Cl_1)$, $n_2(O_2)$, $n_2(O_3)$ with energies, -0.31530, -0.25769, -0.33853a.u and p-characters, 100, 99.98, 99.49% and low occupation numbers, 1.93332, 1.82886, 1.78653 while the lower energy orbitals are: $n_1(Cl_1)$, $n_1(O_2)$, $n_1(O_3)$ with energies -0.91366, -0.68539, -0.54928a.u and p-characters, 17.76, 42.31, 65.56% and high occupation numbers, 1.99367, 1.97728, 1.95025.

Thus, a very close to pure p-type lone pair orbital participates in the electron donation to the $n_1(Cl_1)\rightarrow\sigma^*(C_{24}$-$C_{25})$, $n_2(Cl_2)\rightarrow\sigma^*(C_{24}$-$C_{25})$, $n_3(Cl_3)\rightarrow\pi^*(C_{24}$-$C_{25})$, $n_1(O_2)\rightarrow\sigma^*(C_5$-$C_6)$, $n_2(O_2)\rightarrow\sigma^*(O_3$-$C_5)$, $n_1(O_3)\rightarrow\sigma^*(C_{21}$-$C_{28})$, $n_2(O_3)\rightarrow\pi^*(O_2$-$C_5)$ and $n_1(N_4)\rightarrow\sigma^*(C_6$-$C_7)$ interactions in the compound.

Table 6. The binding affinity values of different poses of the title compound predicted by Autodock Vina.

Mode	Affinity (kcal/mol)	Distance from best mode (Å)	
		RMSD l.b.	RMSD u.b.
1	-7.2	0.000	0.000
2	-7.1	4.683	6.999
3	-7.0	4.506	6.760
4	-6.8	5.111	7.396
5	-6.7	24.457	27.005
6	-6.7	15.112	17.133
7	-6.5	25.883	27.689
8	-6.5	4.666	7.153
9	-6.5	4.599	7.122

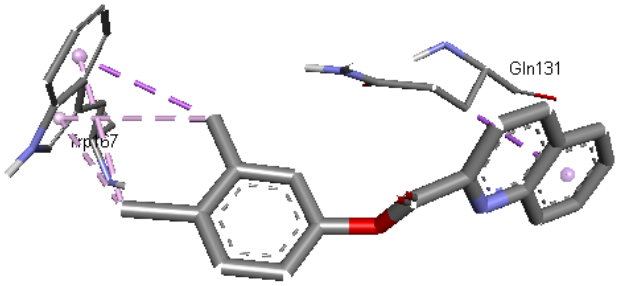

Figure 8. Schematic for the docked conformation of active site of title compound at CDK inhibitors.

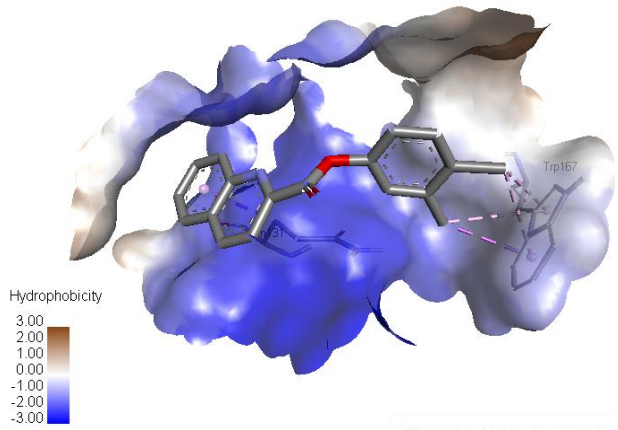

Figure 9. The docked protocol reproduced the co-crystallized conformation with π-alkyl (pink), π-sigma (violet) and hydrophobic receptor surface shown.

4.8. Molecular docking

Quinoline derivatives possess a broad range of bioactivities as such as antibacterial [54], antitumor, anti-HIV-1 integrase, anti-HCV-NS3 helicase and -NS5B-polymerase activities [55-57]. A series of tetracyclic indenoquinolines is used as potential anticancer agents. The compounds, which are obtained through the photoisomerization of Diels–Alder adducts formed between purpurogallin derivatives and nitrosobenzene, have in vitro anti-proliferative activities against breast (MCF-7), lung epithelial (A-549) and cervical (HeLa) adenocarcinoma cells [58]. Several novel functionalized quinolones, which exhibited potential antineoplastic activity against eukaryotic type II topoisomerases [59]. In addition to the antibacterial quinolones, specific members of this drug family display high activity against eukaryotic type II topoisomerases, as well as cultured mammalian cells and invivo tumor models. These antineoplastic quinolones represent an exploitable source of new anticancer agents which might also help addressing undesirable-toxicity and resistance Phenomena [59]. Jayashree et al. reported the molecular docking experiments of 4-oxotheino [3,2-c]quinoline-2-carboxylates with DNA and their potential anticancer property [60]. High resolution crystal structure of CDK inhibitors as anti-cancer was downloaded from the protein data bank website (PDB ID: 2XNB). All molecular docking calculations were performed on Auto Dock-Vina software [61]. The 3D crystal structure of CDK inhibitors was obtained from Protein Data Bank. The protein was prepared for docking by removing the co-crystallized ligands, waters and co-factors. The Auto Dock Tools (ADT) graphical user interface was used to calculate Kollman charges and polar hydrogens. The ligand was prepared for docking by minimizing its energy at B3LYP/6-31g(d) level of theory. Partial charges were calculated by Geistenger method. The active site of the enzyme was defined to include residues of the active site within the grid size of 40Å×40Å×40Å. The most popular algorithm, Lamarckian Genetic Algorithm (LGA) available in Autodock was employed for docking. The docking protocol was tested by extracting co-crystallized inhibitor from the protein and then docking the same. The docking protocol predicted the same conformation as was present in the crystal structure with RMSD value well within the reliable range of 2Å [62]. Amongst the docked conformations, one which binded well at the active site was analyzed for detailed interactions in Discover Studio Visualizer 4.0 software. The ligand binds at the active site of the substrate (Figures 8 and 9) by weak non-covalent interactions. Amino acid Gln131 forms π-sigma interaction with phenyl ring. Trpi67 amino acid forms π-sigma interactions with phenyl ring and π-alkyl interaction with phenyl ring, CH_3 group. The docked ligand title compound forms a stable complex with CDK inhibitors and gives a binding affinity (ΔG in kcal/mol) value of -7.2 (Table 6). These preliminary results suggest that the compound might exhibit inhibitory activity against CDK inhibitors.

5. Conclusions

The optimized molecular structure, vibrational wavenumbers, corresponding vibrational assignments of 4-chloro-3-methylphenyl quinoline-2-carboxylate have been investigated theoretically and experimentally. The geometrical parameters are in agreement with the XRD experimental data. The stability of the title compound arising from hyper-conjugative interaction and charge delocalization has been interpreted using NBO analysis. The HOMO-LUMO analysis

is used to determine the charge transfer within the molecule. From the MEP plot it is clear that the negative regions are over the carbonyl group oxygen atom and hene electrophilic attack can take place in these sites and the positive regions are over the hydrogen atoms hence nucleophilic attack can take place in these regions. From the docking studies, the docked ligand title compound forms a stable complex with CDK inhibitors and gives a binding affinity value of -7.2 kcal/mol and the results suggest that the compound might exhibit inhibitory activity against CDK inhibitors.

Acknowledgements

The authors would like to extend their sincere appreciation to the Deanship of Scientific Research at King Saud University for funding this work through the Research Group Project No.PRG-1436-23.

References

1. S. Kumar, S. Bawa, H. Gupta, Mini Rev. Med. Chem. 9 (2009) 1648.
2. R. Musiol, M. Serda, S. Hensel-Bielowka, J. Polanski, Curr. Med. Chem. 17 (2010) 1960.
3. K. D. Thomas, A. V. Adhikari, S. Telkar, I. H. Chowdhury, R. Mahmood, N. K. Pal, E. Sumesh, Eur. J. Med. Chem. 46 (2011) 5283.
4. K. Kaur, M. Jain, R. P. Reddy, R. Jain, Eur. J. Med. Chem. 45 (2010) 3245.
5. A. Mitchinson, A. Nadin, J. Chem. Soc. Perkin Trans. I 17 (2000) 2862.
6. V. Sridharan, P. Suryavanshi, J. C. Menendez, Chem. Rev. 111 (2011) 7157.
7. R. Vlahov, S. Parushev, J. Vlahov, P. Nickel, G. Snatzke, Pure Appl. Chem. 62 (1990) 1303.
8. M. S. Abdel-Aal, M. S. Morad, Br. Corros. J. 36 (2001) 253.
9. T. P. Hoar, R. D. Holliday, J. Appl. Chem. 3 (1953) 502.
10. B. S. Shylesha, T. V. Venkatesha, B. M. Praveen, K. V. Srinath, Anal. Bioanal. Electrochem. 3 (2011) 249.
11. M. S. Abdel-All, Z. A. Ahmed, M. S. Hassan, J. Appl. Electrochem. 22 (1992) 1104.
12. M. Singh, A. K. Bhattamishra, J. Metallurgy Mater. Sci. 49 (2007) 39.
13. M. Chrzanowdka, M. D. Rozwadowska, Chem. Rev. 104 (2004) 3341.
14. J. D. Scott, R. M. Williams, Chem. Rev. 102 (2002) 1669.
15. V. R. Solomon, H. Lee, Eur. J. Pharmacol. 25 (2009) 220.
16. P. Hewawasam, W. Fan, J. Knipe, S. L. Moon, C. G. Boissard, V. K. Gribkoff, J. E. Starztt, Bioorg. Med. Chem. Lett. 12 (2002) 1779.
17. D. S. Raja, N. S. P. Bhuvanesh, K. Natarajan, Eur. J. Med. Chem. 46 (2011) 4584.
18. D. S. Raja, N. S. P. Bhuvanesh, K. Natarajan, Inorg. Chem. 50 (2011) 12852.
19. R. T. Ulahannan, C. Y. Panicker, H. T. Varghese, C. Van Alsenoy, R. Musiol, J. Jampilek, P. L. Anto, Spectrochim. Acta 121 (2014) 445.
20. R. T. Ulahannan, C. Y. Panicker, H. T. Varghese, C. Van Alsenoy, R. Musiol, J. Jampilek, P. L. Anto, Spectrochim. Acta 121 (2014) 404.
21. R. T. Ulahannan, C. Y. Panicker, H. T. Varghese, R. Musiol, J. Jampilek, C. Van Alsenoy, J. A. War, A. A. Al-Saadi, Spectrochim. Acta 151 (2015) 335.
22. R. T. Ulahannan, C. Y. Panicker, H. T. Varghese, R. Musiol, J. Jampilek, C. Van Alsenoy, J. A. War, S. K. Srivastava, Spectrochim. Acta 151 (2015) 184.
23. E. Fazal, C. Y. Panicker, H. T. Varghese, S. Nagarajan, B. S. Sudha, J. A. War, S. K. Srivastava, B. Harikumar, P. L. Anto, Spectrochim. Acta 143 (2015) 213.
24. E. Fazal, C. Y. Panicker, H. T. Varghese, S. Nagarajan, B. S. Sudha, J. A. War, S. K. Srivastava, B. Harikumar, P. L. Anto, Spectrochim. Acta 145 (2015) 260.
25. S. Shahab, H. A. Almodarresiyeh, R. Kumar, M. Darroudi, J. Mol. Struct. 1088 (2015) 105.
26. O. V. Dyablo, A. F. Pozharskii, E. A. Shmoilova, V. A. Ozeryanskii, N. S. Fedik, K. Y. Suponitsky, J. Mol. Struct. 1107 (2016) 305.
27. J. E. Nycz, K. Czyz, M. Szala, J. G. Malecki, G. Shaw, B. Gilmore, M. Jon, J. Mol. Struct. 1106 (2016) 416.
28. E. Fazal, P. S. Murthy, K. A. Naidu, A. Maheshwaraiah, S. Nagarajan, B. S. Sudha, Microwave assisted synthesis and biological evaluation of potential quinoline-2-carboxylates of aromatic compounds, Indo Am. J. Pharm. Res. 2 (2015) 625.
29. E. Fazal, M. Kaur, B. S. Sudha, S. Nagarajan, J. P. Jasinski, Acta Cryst. E 69 (2013) o1842.
30. M. J. Frisch, G. W. Trucks, H. B. Schlegel, G. E. Scuseria, M. A. Robb, J. R. Cheeseman, G. Scalmani, V. Barone, B. Mennucci, G. A. Petersson, H. Nakatsuji, M. Caricato, X. Li, H. P. Hratchian, A. F. Izmaylov, J. Bloino, G. Zheng, J. L. Sonnenberg, M. Hada, M. Ehara, K. Toyota, R. Fukuda, J. Hasegawa, M. Ishida, T. Nakajima, Y. Honda, O. Kitao, H. Nakai, T. Vreven, J. A. Montgomery, Jr., J. E. Peralta, F. Ogliaro, M. Bearpark, J. J. Heyd, E. Brothers, K. N. Kudin, V. N. Staroverov, T. Keith, R. Kobayashi, J. Normand, K. Raghavachari, A. Rendell, J. C. Burant, S. S. Iyengar, J. Tomasi, M. Cossi, N. Rega, J. M. Millam, M. Klene, J. E. Knox, J. B. Cross, V. Bakken, C. Adamo, J. Jaramillo, R. Gomperts, R. E. Stratmann, O. Yazyev, A. J. Austin, R. Cammi, C. Pomelli, J. W. Ochterski, R. L. Martin, K. Morokuma, V. G. Zakrzewski, G. A. Voth, P. Salvador, J. J. Dannenberg, S. Dapprich, A. D. Daniels, O. Farkas, J. B. Foresman, J. V. Ortiz, J. Cioslowski, D. J. Fox, Gaussian 09 (Revision B. 01), Gaussian, Inc., Wallingford CT (2010).
31. A. J. Austin, R. Cammi, C. Pomelli, J. W. Ochterski, R. L. Martin, K. Morokuma, V. G. Zakrzewski, G. A. Voth, P. Salvador, J. J. Dannenberg, S. Dapprich, A. D. Daniels, O. Farkas, J. B. Foresman, J. V. Ortiz, J. Cioslowski, D. J. Fox, Gaussian 09 (Revision E. 01), Gaussian, Inc, Wallingford CT (2010).
32. J. B. Foresman, Exploring Chemistry with Electronic Structure Methods: A Guide to Using Gaussian, Gaussian Inc., Pittsburg, PA (1996).
33. R. Dennington, T. Keith, J. Millam, GaussView (Version 5), Semichem Inc., Shawnee Mission KS (2009).
34. J. M. L. Martin, C. Van Alsenoy, GAR2PED, A Program to Obtain a Potential Energy Distribution from a Gaussian Archive Record, University of Antwerp, Belgium (2007).
35. A. F. Holleman, E. Wiberg, N. Wiberg, Lehrburch der Anorganischen Chemie, Walter de Gruyter, Berlin (2007).
36. N. P. G. Roeges, A Guide to the Complete Interpretation of Infrared Spectra of Organic Structures, Wiley, New York (1994).
37. G. Varsanyi, Assignments for Vibrational Spectra of Seven Hundred Benzene Derivatives, Wiley, New York (1974).
38. M. Kaur, Y. S. Mary, H. T. Varghese, C. Y. Panicker, H. S. Yathirajan, M. S. Siddegowda, C. Van Alsenoy, Spectrochim. Acta 98 (2012) 91.
39. V. S. Madhavan, H. T. Varghese, S. Mathew, J. Vinsova, C. Y. Panicker, Spectrochim. Acta 72 (2009) 547.
40. K. C. Mariamma, H. T. Varghese, C. Y. Panicker, K. John, J. Vinsova, C. Van Alsenoy, Spectrochim. Acta 112 (2013) 161.
41. R. M. Silverstein, G. C. Bassler, T. C. Morri, Spectrometric Identification of Organic Compounds (5th ed.), John Wily and Sons Inc., Singapore (1991).
42. G. Socrates, Infrared Characteristic Group Frequencies, Wiley, New York (1980).

43. A. Karton, M. A. Iron, M. E. van der Boom, J. M. L. Martin, J. Phys. Chem. A 109 (2005) 5454.
44. Y. Sun, X. Chen, L. Sun, X. Guo, W. Lu, Chem. Phys. Lett. 381 (2003) 397.
45. O. Christiansen, J. Guass, J. F. Stanton, Chem. Phys. Lett. 305 (1999) 147.
46. C. Adant, M. Dupuis, J. L. Bredas, Int. J. Quantum Chem. 56 (2004) 497.
47. A. Gul, Z. Akhter, R. Qureshi, A. S. Bhatti, RSC Adv. 4 (2014) 22094.
48. A. Gul, Z. Akhter, M. Siddiq, R. Qureshi, A. S. Bhatti, J. Appl. Polym. Sci. 131 (2014) 40698.
49. P. Thul, V. P. Gupta, V. J. Rama, P. Tandon, Spectrochim. Acta 75 (2010) 251.
50. S. Sert, H. Sreenivasa, K. E. Dogan, P. A. Manojkumar, Suchetan, F. Ucun, Spectrochim. Acta 127 (2014) 122.
51. K. Chaitanya, Spectrochim. Acta 86 (2012) 159.
52. A. Jayaprakash, V. Arjunan, S. Mohan, Spectrochim. Acta 81 (2011) 620.
53. R. J. Parr, R. G. Pearson, J. Am. Chem. Soc. 105 (1983) 7512.
54. E. D. Glendening, A. E. Reed, J. E. Carpenter, F. Weinhold, NBO (Version 3. 1), Gaussian Inc., Pittsburg, PA (2003).
55. V. E. Anderson, N. Osheroff, Curr. Pharm. Des. 7 (2001) 337.
56. A. Ahmed, M. Daneshtalab, J. Pharm. Pharm. Sci. 15 (2012) 52.
57. C. Mugnaini, S. Pasquini, F. Corelli, Curr. Med. Chem. 16 (2009) 1746.
58. S. Richter, C. Parolin, M. Palumbo, G. Palu, Curr. Drug Targets Infect. Disord. 4 (2004) 111.
59. S. Chakrabarty, M. S. Croft, M. G. Markob, G. Moyna, Bioorg. Med. Chem. 21 (2013) 1143.
60. C. Sissi, M. Palumbo, Curr. Med. Chem. Anticancer Agents 3 (2003) 439.
61. A. Jayashree, Y. Satish, M. A. Reddy, Int. J. Res. Pharm. Biomed. Sci. 4 (2013) 607.
62. O. Trott, A. J. Olson, J. Comput. Chem. 31 (2010) 455.
63. B. Kramer, M. Rarey, T. Lengauer, Proteins: Struct. Funct. Genet. 37 (1999) 228.

Cite this article as:

Fazal Edakot *et al.*: **Synthesis, spectroscopic analysis and molecular docking studies of 4-chloro-3-methylphenyl quinoline-2-carboxylate.** Sci. Lett. J. 2016, **5**: 237